Korean J. Chem. Eng., 36(8), 1350-1359 (2019)
DOI: 10.1007/s11814-019-0291-1

pISSN: 0256-1115
eISSN: 1975-7220

Optimization of inhibitive action of sodium molybdate (VI) for corrosion of carbon steel in saline water using response surface methodology

Khalid Hamid Rashid* and Anees Abdullah Khadom,†**

*Department of Chemical Engineering, University of Technology, Baghdad, Iraq
**Department of Chemical Engineering, College of Engineering, University of Diyala, Diyala, Iraq
(*Received 25 January 2019 • accepted 1 May 2019*)

Abstract–The performance of sodium molybdate (Na_2MoO_4) (VI) as a corrosion inhibitor for medium carbon steel corrosion in saline water containing nitrate and chloride ions was studied at various inhibitor concentrations, temperatures, exposure times and rotational velocities. Mass loss and electrochemical techniques were used to evaluate the corrosion rates. The individual and interactive effects of these four parameters were optimized for minimum response of corrosion rate using central composite design (CCD) with response surface methodology (RSM). Nonlinear regression strategy in light of Gauss-Newton technique was utilized for modeling and optimization of the corrosion inhibition experiments. Second-order polynomial model was suggested to predict the corrosion rates as a function of four variables. The individual effect of temperature on corrosion rate was higher than the individual effects of inhibitor concentration, exposure time and rotational velocity, respectively. The interaction effects of independents variables were also addressed. Open circuit potential measurements were used as a significant way to gain information about the behavior of steel corrosion. Steady state potential was reached after one hour of immersion time. Mass loss results were in a good agreement with potentiodynamic polarization technique. Optimum inhibition efficiency was 95.9% at optimum operating conditions. Polarization plots revealed that the inhibitor acts as the anodic-type inhibitor.

Keywords: Corrosion, Optimization, Inhibition, Mass Loss, Saline Water

INTRODUCTION

Medium carbon steel (MC-steel), because of its great mechanical properties and low production costs, is in wide usage in various fields of industry [1,2]. Unfortunately, MC-steel suffers from corrosion problems when contacted with aggressive solutions [3]. Saline solutions are one of the harmful environments that affect steel corrosion resistance. Besides the high salts content in saline solutions there are other common factors that influence the metallic corrosion rates. Temperature, flow velocity and time of exposure are some examples of issues that may affect the corrosion rate of a given metal in saline solutions. The changes in temperature have a significant effect on the corrosion process. Corrosion rate in diffusion control process is doubled for a certain increase in temperature, while in activation process may be increased by 10-100 times depending on the magnitude of the activation energy [4]. Increasing solution temperature leads to decreasing viscosity of solution with a consequent increase in oxygen diffusivity, which leads to increase the rate of mass transfer of dissolved oxygen to the cathode surface, then increasing the corrosion rate. On the other hand, the decrease in saline water viscosity with increasing temperature improves the saline water conductivity with a consequent increase in the rate of corrosion [5]. Generally, the dissolution rate of steel increases with the increasing of the flow rate. This may be attributed to a decrease in the thickness of hydrodynamic boundary layer and diffusion layer across which dissolved oxygen diffuses and other corrosive species to the metal surface. With the consequent increase in the diffusion rate of oxygen, the resistance of surface film nearly vanishes, the corrosion products, depolarization of oxygen, and protective film are continuously swept away and continuous corrosion happens [6]. The exposure time is another important factor and the corrosion rate may increase with time [5].

Corrosion of metals can be controlled using different methods. Inhibitors represent one of these corrosion control techniques that can be classified according to chemical structure and mechanism of action [7-10]. Synthesis and natural organic inhibitors are widely used as safe, cheap and environmentally friendly materials. In contrast, most inorganic inhibitors are dangerous and poisoning, such as nitrites, arsenates, chromates [11]. Although molybdate is one of the inorganic corrosion inhibitors, it can be used with nonhazardous effects [12]. The inhibition impact of sodium molybdate (SM) for the carbon steel protection corrosion in saline solution has been reported in many research works [13-15]. Most of literature works in the field of corrosion control focused on corrosion mechanism, type and performance of inhibitor, kinetics studies, etc. Optimization, statistical and mathematical studies received less attention. In chemistry, the optimization procedure is a standout amongst the most well-known applications. The principal target of optimization is to decide the levels of free factors that prompt a minimum (or a maximum) estimation of an outcome. This methodology can be achieved in two diverse means: multivariate and univariate. Multivariate procedures are statistical techniques that measure connections among factors. In customary univariate techniques, the analyses are led keeping every one of the factors consistent with the excep-

†To whom correspondence should be addressed.
E-mail: aneesdr@gmail.com

tion of the variable whose impact is being considered. In any case, it does not demonstrate what might happen if different factors are altered. The consolidated impact of factors can be anticipated, which is virtually tricky in conventional experimentation [16]. Recently, multivariate methods have been utilized repeatedly for studies of optimization in science, engineering, and manufacturing, taking into account their points of interest, for example, the prerequisite of less time, experimental work, and reagents. Thus, they are speedier and more financially savvy than conventional univariate approaches just utilized to optimize one test variable at once, keeping consistent the staying ones. Response surface methodology (RSM) is utilized generally as an exact modeling of multivariate method to evaluate graphically the connection between response and various experimental variables for optimization process RSM comprises of a set of mathematical and statistical techniques. One of the RSM fundamental aims is to decide the optimum settings of the control factors that result in a maximum (or a minimum) response above a specific interest area. It attempts to analyze the impact of the free factors on a particular dependent variable (response), either exclusively or on the whole. The design of experiment (DoE) studies the effects of interactions of the process factors leading to the establishment of a model correlating the process (independent parameters) with the corrosion rate (response parameter). The usual one factor at a time (OFAT) method of analysis fails to account for the interaction effects between all factors, and therefore a greater number of experimental runs are needed.

Central composite design (CCD) is a common method for response surface methodology (RSM) in the design of experiments that is appropriate for a quadratic surface model and for corrosion process optimization. Central composite design (CCD) exhibited by Box and Wilson is a second-order multivariate plan method that permits the assurance of both quadratic and linear models. The total number of experiments in the CCD can be calculated based on both the number of independent variables and the number of repetitions of the central points. So, CCD consists of three different sets of experimental points. The factorial design in the variables studied (each variable having two levels), the set of center points (this point is frequently replicated to improve the experiment precision), and the set of axial points (experimental runs like to the center points except for one variable that takes on values both above and below the median of the two factorial levels) [17,18].

The analysis of the optimum corrosion inhibition treatment factors, temperature and sodium dodecyl benzene sulfonate (SDBS) concentration on aluminum corrosion rate in hydrochloric acid (HCl) solution was studied by Deniz and Sibel [19] by utilizing the methodology of response surface RSM with design of central composite CCD. Nine experiments were designed using CCD and they found the lowest corrosion current i_{corr} was obtained at SDBS concentration at high level and temperature at lowest level. Khadom and Rashid [20] studied the application of central composite rotatable Box-Wilson experimental design (BWED). The optimum conditions of steel corrosion in HCl solution in absence and presence of kiwi juice as green corrosion inhibitor were evaluated successfully. The objective of this work is to investigate the inhibitive activity of SM (VI) and other operating parameters (temperature, rotational velocity and exposure time) on the rate of corrosion of MC-steel alloy in the saline solution containing nitrate and chloride ions under optimum inhibition conditions using CCD with RSM.

EXPERIMENTAL WORK

1. Corrosive Solution, Material and Samples

Aerated saline water containing nitrate and chloride ions were used as a corrosive solution. Sodium molybdate, Na_2MoO_4 (VI) (99.5% purity) was used as a corrosion inhibitor. Corrosion rate of carbon steel in presence and absence of sodium molybdate Na_2MoO_4 (VI) in a concentrations of 7, 7.5, 8, 8.5 and 9 ppm/(0.5 M $NaNO_3$ and 0.5 M NaCl solution), at various temperatures (10, 30, 50, 70 and 90 °C), various exposure times (2, 4, 6, 8 and 10 h), and various rotational velocities (1,000, 1,125, 1,250, 1,375 and 1,500 rpm) was optimized. Weight loss and potentiodynamic polarization methods were used for corrosion rate evaluation. Analar benzene (C_6H_6 of 98.9% purity) and analar acetone (C_3H_6O of 99.5% purity) were utilized for cleaning and drying the samples. The specimen dimensions were 2.07 cm long, 2 cm outside diameter, and 0.12 cm thickness with an overall area of surface approximated to 13 cm^2. The material of the working electrode used was a medium carbon steel alloy with chemical composition (wt%) of 0.337 C, 0.046 S, 0.163 Si, 0.053 P, 0.102 Ni, 0.813 Mn, 0.178 Cr, 0.018 Mo, 0.004 V, 0.002 W, 0.36 Cu and the balance is iron.

2. Weight Loss Measurements

Steel specimens were cleaned by washing with cleanser and flushed with tap water, then by deionized water, degreased by analar C_6H_6 and C_2H_6O. Steel samples were annealed in a vacuum furnace at 600 °C for one hour and cooled under vacuum to 25 °C. Then, the samples were kept in a desiccator over a silica gel. Before each test, medium carbon-steel was abraded with sandpaper of grade number 220, 320, 400 and 600. Then, the samples were washed with running tap water, and by deionized water, dried with clean tissue, degreased with C_6H_6, dried, degreased with C_2H_6O, dried, left to dry for one hour in a desiccator over silica gel. Measurement of weight loss is probably the most widely used method to measure corrosion rate. Samples were accurately weighted to the fourth decimal of gram and dimensions were measured with a Vernier to the second decimal of millimeter. Steel samples were immersed completely in corrosive solution of 2,500 cm^3 size contained in a conical flask for a specific period of time at the desired inhibitor concentration and temperature. Mass losses in $gm \cdot m^{-2} \cdot day^{-1}$ (gmd) were evaluated in absence and presence of sodium molybdate as a corrosion inhibitor. Tests were in a standard glass cell. The cell was equipped with six necks, but only three necks were used: One for the working sample (MC-steel ring), one for the thermometer, and one for the condenser. The other necks were plugged with a rubber stopper. The specimen was hung on a rotating Teflon shaft at specific conditions. After that, the specimen was cleaned, washed with flowing tap water using a brush to remove the corrosion products, washed with deionized water, dried with the clean tissue, degreased with C_6H_6, dried, degreased with C_2H_6O, dried, left for one hour, then the weight loss was recorded.

3. Multivariate Optimization Strategy

The multivariate optimization was done using central composite matrix design (CCD) and the developed data were used in

Table 1. Corrosion inhibition factors and their real and coded levels

Independent factors	Levels of factors				
	Lowest −2	Low −1	Centre 0	High +1	Highest +2
A: Temperature (°C)	10	30	50	70	90
B: Inhibitor conc. (ppm)	7	7.5	8	8.5	9
C: Rotational velocity (rpm)	1000	1125	1250	1375	1500
D: Exposure time (h)	2	4	6	8	10

STATISTICA software program. Experimental design is a way for systematically changing the controllable input parameters and monitoring the influences of these parameters on the result of output factors. The utilizing of supposition in our investigation was that the input parameters singular impacts on the output factors product are divisible. That implies the independent parameter's influence on the execution variable does not rely upon some other free parameter for diverse level settings. Before directing of the experiment, the learning of the product/process under study is of prime significance in recognizing the variables inclined to impact the result. With a specific end goal to arrange an exhaustive rundown of variables, the contribution to the experiment is by and large acquired from the specialists engaged with the venture. The goal of this examination was to deliver the corrosion inhibition with the minimum corrosion rate. The temperature, inhibitor concentration, rotational velocity and exposure time were chosen as the controllable information parameters for our situation. Once the free parameters are chosen, the number of levels for each factor must be chosen. The range of operating parameters (temperature, time, inhibitor concentration and velocity) was in the range of values available in the literature [4-7]. The determination of various levels relies upon how the result (corrosion rate for our situation) is influenced because of various level settings. On the off chance that the result is a straight capacity of the chosen parameter, at that point the quantity of level setting will be two. However, if the parameter is not straightly related, at that point one could go to more elevated levels. A relationship between the corresponding real factors and the coded one was constructed as follows:

$$x_{coded}=\frac{x_{real}-x_{center}}{\frac{x_{center}-x_{lowest}}{\sqrt{k}}} \quad (1)$$

where k represents the number of variables. Tarantino [21] proposed that the coded factors take a value between 2 and −2 as per the central composite rotatable. The range of temperature was 10-90 °C, inhibitor concentration range 7-9 ppm, rotational velocity 1,000-1,500 rpm and exposure time range 2-10 h. The expressions of level in the coded form for the system are evaluated from Eq. (1):

$$x_1=\frac{T-50}{20},\ x_2=\frac{C_{Na_2MoO_4}-8}{0.5},\ x_3=\frac{\omega-1250}{125},\ x_4=\frac{t-6}{2} \quad (2)$$

where $C_{Na_2MoO_4}$ is inhibitor concentration (ppm), T is temperature of saline water (°C), ω is rotational velocity (rpm) and t is exposure time (h) studied at two levels. The relationship between the corresponding real factors and coded level is shown in Table 1. Normally, in the case of four parameters with two levels and repeated experiments of the center's conditions four times, $2^4+2\times4+4$ yields 28 runs. Experimental design of Box-Wilson is not difficult to apply to numerous engineering cases, making it one of strongest and easiest tool for arrangement of tests and describing a physical mechanism. These experiments' arrangement was efficiently used to develop process mathematical models [22-24]. For four variables, the second-order quadratic model can be represented as follows:

$$y_p=a_o+a_1x_1+a_2x_2+a_3x_3+a_4x_4+a_5x_1^2+a_6x_2^2+a_7x_3^2+a_8x_4^2 +a_9x_1x_2+a_{10}x_1x_3+a_{11}x_1x_4+a_{12}x_2x_3+a_{13}x_2x_4+a_{14}x_3x_4 \quad (3)$$

where y_p is predicted corrosion rate (gmd), $x_1$is temperature (°C), x_2 is inhibitor concentration (ppm), x_3 is rotational velocity (rpm), x_4 is exposure time (h) and a_o, a_1, …, a_{14} are constants. It is clear that the quadratic model takes into account the individual effect of each variable and the interaction effect between them, which makes it more preferred than other models.

4. Open-circuit Potential Measurements

The open circuit potential (OCP) analysis was evaluated in the system shown in Fig. 3. The extent of the working electrode potential was registered as a function of time against saturated calomel electrode (SCE) bridged by a lugging Haber Probe. The testing strategy is proficient by setting the lugging Haber capillary at a space of 2 mm from the working electrode. The potential of open-cell can be inspected directly using a voltmeter. Initially for 40 minutes, the corrosion potential was estimated every 3 minutes, and then every 30 minutes a reading was taken by a digital voltmeter until reaching the steady state conditions [25].

5. Potentiodynamic Polarization Measurements

The measurement was performed in aerated, saline water containing 0.5 M nitrate and 0.5 M chloride ions (0.5 M $NaNO_3$ and 0.5 M NaCl) at optimum conditions acquired from mass loss technique in absence and presence of sodium molybdate (SM) as a corrosion inhibitor using potentiodynamic polarization technique. Polarization measurement is probably the most used method for studying the corrosion behavior of a metal in corrosive media. Metallic surfaces can be polarized by the application of an external voltage which causes current flows between anode and cathode caused a change in the electrode potential. This change, termed as polarization, affects the rate of corrosion. The test was done using a standard polarization glass cell spherical flat bottom flask of 2,500 cm^3. The cell has six necks; five of these necks were used. One for the steel sample that acts as a working electrode (MC-steel cylinder), One had a tube-shaped gap for the lugging Haber probe mounting that acts as a reference standard calomel electrode (SCE), one

for the thermometer, one for the auxiliary graphite electrode, one for the condenser. The other neck was plugged with a rubber stopper. The working electrode was (2 cm outside diameter×2.07 cm long) MC-steel alloy cylinder specimens; this cylinder was fixed on the brass zone on the shaft. Graphite electrode was utilized as an auxiliary electrode has a measurement of (1.5 cm diameter×4 cm long); a wire was associated with graphite electrode. The electrode was mounted specifically to the working electrode. To ensure a saturated potassium chloride solution, a small amount of potassium chloride (solid) was kept in the solution of calomel electrode during the test. Samples readiness was completed as in weight loss method portrayed beforehand. The cell and electrodes were washed with running tap water, then, by distilled water and then by saline water. The cell was fitted in a water bath for an appropriate time until reaching thermal equilibrium (i.e., temperature inside the cell equal to the temperature of the water bath). The auxiliary and reference electrodes were fitted and dipped into the corrosive media. An electrical connection was made among the electrodes. All corrosion cell parts were fixed and connected to power supply, resistors, voltmeter and ammeter. Cathodic polarization was started from low potential of −1,000 mV until reaching the corrosion potential, and then the connection to the power supply was inverted and continued with anodic polarization up to 600 mV. The potential was changed by a step approximately equal to 10 to 15 mV per minute and the current density was recorded.

RESULTS AND DISCUSSION

1. Mass Loss Measurements Regression Analysis

Corrosion rate of MC-steel in saline water containing 0.5 M $NaNO_3$ and 0.5 M NaCl ions in presence and absence of various concentrations of sodium molybdate (SM) as a corrosion inhibitor at different rotational velocities, temperatures and exposure times was studied by weight loss measurements. The corrosion rate of MC-steel was determined using the following formula:

$$C.R = \frac{\text{Weightloss (g)}}{\text{Area (m}^2\text{)} \times \text{time (day)}} \quad (4)$$

where C.R represent the corrosion rate in g/m^2·day (gmd). Table 2 shows the results of nonlinear regression analysis. Temperature,

Table 2. Experimental design of the independent factors against experimental and predicted response

Exp. No.	Coded parameters				Real parameters				Experimental C.R	Predicted C.R	Root-mean-square error (RMSE)
	x_1	x_2	x_3	x_4	T (°C)	$C_{Na_2MoO_4}$ (ppm)	ω (rpm)	t (h)	$C.R_E$ (gmd)	$C.R_P$ (gmd)	
1.	−1	−1	−1	−1	30	7.5	1125	4	7.55	8.88	0.252
2.	1	−1	−1	−1	70	7.5	1125	4	20.04	18.46	0.299
3.	−1	1	−1	−1	30	8.5	1125	4	35.67	32.35	0.629
4.	1	1	−1	−1	70	8.5	1125	4	21.71	21.67	0.008
5.	−1	−1	1	−1	30	7.5	1375	4	18.56	18.97	0.077
6.	1	−1	1	−1	70	7.5	1375	4	43.48	38.57	0.932
7.	−1	1	1	−1	30	8.5	1375	4	15.34	20.13	0.909
8.	1	1	1	−1	70	8.5	1375	4	25.04	19.46	1.058
9.	−1	−1	−1	1	30	7.5	1125	8	16.17	17.24	0.203
10.	1	−1	−1	1	70	7.5	1125	8	40.43	34.85	1.058
11.	−1	1	−1	1	30	8.5	1125	8	20.35	24.47	0.781
12.	1	1	−1	1	70	8.5	1125	8	26.73	21.81	0.934
13.	−1	−1	1	1	30	7.5	1375	8	25.07	24.32	0.142
14.	1	−1	1	1	70	7.5	1375	8	53.13	51.94	0.226
15.	−1	1	1	1	30	8.5	1375	8	12.17	9.24	0.556
16.	1	1	1	1	70	8.5	1375	8	18.71	16.59	0.402
17.	−2	0	0	0	10	8	1250	6	18.27	13.25	0.952
18.	2	0	0	0	90	8	1250	6	19.90	30.19	1.952
19.	0	−2	0	0	50	7	1250	6	20.81	23.75	0.558
20.	0	2	0	0	50	9	1250	6	9.54	11.87	0.442
21.	0	0	−2	0	50	8	1000	6	22.67	24.47	0.342
22.	0	0	2	0	50	8	1500	6	25.88	29.35	0.658
23.	0	0	0	−2	50	8	1250	2	23.77	25.55	0.337
24.	0	0	0	2	50	8	1250	10	27.55	31.04	0.662
25.	0	0	0	0	50	8	1250	6	7.77	7.65	0.022
26.	0	0	0	0	50	8	1250	6	7.80	7.65	0.028
27.	0	0	0	0	50	8	1250	6	7.56	7.65	0.017
28.	0	0	0	0	50	8	1250	6	7.49	7.65	0.031

inhibitor concentration, rotational velocity and exposure time were considered in the development of the mathematical model for the corrosion inhibition rate. Eq. (3) represents the interaction between the variables and the individual effect of each variable. *STATISTICA* 10 software was used to derive the model using nonlinear estimation method. The model in terms of real variables can be written as shown below with correlation coefficient of 0.95:

$$\begin{aligned} C.R_{p(W.L)} = & -6.59+1.83T-7.24C_{Na_2MoO_4}-0.07\omega+18.94t+0.008T^2 \\ & +10.16C^2_{Na_2MoO_4}+0.0003\omega^2+1.29t^2-0.51TC_{Na2MoO4}+0.001T\omega \\ & +0.05Tt-0.08C_{Na_2MoO_4}\omega-4.06C_{Na_2MoO_4}t-0.003\omega t \end{aligned} \quad (3a)$$

where $C.R_{P(W.L)}$ is the predicted weight loss corrosion rate ($g/m^2 \cdot day$). The model in coded form can be written as:

$$\begin{aligned} C.R_{p(W.L)} = & 7.65+4.23x_1-2.96x_2+1.21x_3+1.37x_4+3.51x_1^2 \\ & +2.54x_2^2+4.81x_3^2+5.16x_4^2-5.06x_1x_2+2.5x_1x_3 \\ & +2.01x_1x_4-5.57x_2x_3-4.06x_2x_4-0.75x_3x_4 \end{aligned} \quad (3b)$$

The predicted corrosion rate was in a good agreement with experimental one and the root-mean-square error (RMSE) was relatively low.

Eq. (3b) can be optimized for minimum corrosion rate. The first-order derivative of Eq. (3b) can be obtained and equated to zero to yield the following partial derivatives:

$$\begin{aligned} \frac{\partial y_p}{\partial x_1} &= a_1+2a_{11}x_1+a_{12}x_2+a_{13}x_3+a_{14}x_4=0 \\ \frac{\partial y_p}{\partial x_2} &= a_2+2a_{22}x_2+a_{12}x_1+a_{23}x_3+a_{24}x_4=0 \\ \frac{\partial y_p}{\partial x_3} &= a_3+2a_{33}x_3+a_{13}x_1+a_{23}x_2+a_{34}x_4=0 \\ \frac{\partial y_p}{\partial x_4} &= a_4+2a_{44}x_4+a_{14}x_1+a_{24}x_2+a_{34}x_3=0 \end{aligned} \quad (5)$$

Arrangement of Eq. (5):

$$\begin{aligned} 2a_{11}x_1+a_{12}x_2+a_{13}x_3+a_{14}x_4 &= -a_1 \\ a_{12}x_1+2a_{22}x_2+a_{23}x_3+a_{24}x_4 &= -a_2 \\ a_{13}x_1+a_{23}x_2+2a_{33}x_3+a_{34}x_4 &= -a_3 \\ a_{14}x_1+a_{24}x_2+a_{34}x_3+2a_{44}x_4 &= -a_4 \end{aligned} \quad (6)$$

Eq. (6) can be solved easily via Cramer's rule. Optimum conditions in terms of real and coded variables are shown in Table 3.

The optimum $C.R_p$ at optimum levels of x_1, x_2, x_3 and x_4 was 9.21 gmd. However, this optimum value has veered off from minimum $C.R_p$ in Table 2. This may be ascribed to the fact that Eq. (3) considers the interaction and individual influences of free factors. While, experimental data performed at particular conditions. Working at the high level of concentration of inhibitor and exposure time, the center level of rotational velocity, and lower level of temperature gave a minimum inhibited $C.R_p$ of 9.21 gmd. The higher level of concentration of inhibitor improved the likelihood of adsorption of more SM molecules on steel surface. The center level of rotational velocity reduces corrosion attack depending on its influence on the corrosion mechanism involved between the surface metal and environment to which it is exposed. The higher level of exposure time increases the chance of covering more areas on the surface of the metal. While, dealing with the lower level of temperature diminishes the reaction rate of metal dissolution. The linear coefficients (a_1, a_2, a_3 and a_4) of the operating free factors (x_1, x_2, x_3 and x_4) were 4.23, −2.96, 1.21, and 1.37, respectively. These demonstrate that the influence of each factor on inhibiting $C.R_p$ can be ordered as $x_1>x_2>x_4>x_3$ and $C.R_p$ is exceedingly influenced by temperature, then inhibitor concentration and the exposure time and to less extent by rotational velocity.

Table 3. Minimum corrosion rate and optimum values of variables (factors)

Corrosion parameters	Optimum values (medium carbon steel alloy)	
	Coded	Real
Temperature (°C)	−0.610	40.27
Na_2MoO_4 (VI) Concentration (ppm)	−0.002	8.09
Rotational Velocity (rpm)	0.029	1257.45
Exposure Time (h)	−0.012	6.08
Function minimum (corrosion rate, gmd)	9.21	

The variance analysis (F-test) can be utilized for testing the significance of each influence in the model [23]. The variance of coefficients (S_r^2 and S_b^2) [24] is calculated using Eqs. (7) and (8), and the results are shown in Table 4.

$$S_r^2 = \Sigma\frac{\varepsilon_i^2}{\gamma} \quad (7)$$

$$S_b^2 = \frac{S_r^2}{\Sigma x^2} \quad (8)$$

where γ is degree of freedom that represents the difference between number of experiments and number of coefficients.

The results of Table 4 show that most of the interaction and individual influences of factors are significant and must be considered. According to ANOVA analysis, the insignificant terms of model 3b were removed and the new response model can be written as follows:

Table 4. Results of analysis of variance (ANOVA)

Factor evaluated	Σx^2	Estimated factor (b)	Variance S_b^2	F-value $=b^2/S_b^2$	$F_{0.95(1,13)}$ =4.67
b_1	24	4.23	1.1475	15.5929	S
b_2	24	−2.96	1.1475	7.6354	S
b_3	24	1.21	1.1475	1.2759	NS
b_4	24	1.37	1.1475	1.6356	NS
b_{11}	48	3.51	0.5737	21.4748	S
b_{22}	48	2.54	0.5737	11.2456	S
b_{33}	48	4.81	0.5737	40.3279	S
b_{44}	48	5.16	0.5737	46.4103	S
b_{12}	16	−5.06	1.7212	14.8754	S
b_{13}	16	2.50	1.7212	3.6312	NS
b_{14}	16	2.01	1.7212	2.3473	NS
b_{23}	16	−5.57	1.7212	18.0252	S
b_{24}	16	−4.06	1.7212	9.5768	S
b_{34}	16	−0.75	1.7212	0.3268	NS

$$C.R_{p(W.L)}=7.65+4.23x_1-2.96x_2+3.51x_1^2+2.54x_2^2+4.81x_3^2 +5.16x_4^2-5.06x_1x_2-5.57x_2x_3-4.06x_2x_4 \quad (3c)$$

The main variables of rotational velocity and exposure time and the interaction between temperature and rotational velocity (x_1, x_3), temperature and exposure time (x_1, x_4) and rotational velocity and exposure time (x_3, x_4) were insignificant. The relation between predicted and experimental corrosion rate is shown in Fig. 1. The negative sign for the SM concentration parameter demonstrates that the corrosion rate increases with the increase in the inhibitor concentration. The positive sign for the parameters of the temperature, rotational velocity and exposure time indicates that the corrosion rate decreases with the increase in these three factors. Fig. 2 represents a Pareto chart for MC-steel in saline water containing nitrate and chloride ions, which suggests that the prevailing process factor is the temperature, while the effects of the inhibitor concentration, rotational velocity and exposure time are impressively smaller. The interaction parameters ($C_{Na_2MoO_4}\times\omega$), (T, $C_{Na_2MoO_4}$) and the quadratic parameter (t^2, ω^2) have significant influence.

2. Influence of Independent Variables on Corrosion Rate

The effects of independent variables on the inhibited corrosion rate of MC-steel in a saline solution containing nitrate and chloride ions 0.5 M $NaNO_3$ & 0.5 M NaCl at various inhibitor concentrations of sodium molybdate are shown in Table 2. Eq. (3a) or (3b) represents a significant relationship between the dependent variable (corrosion rate) and independent variables with high correlation

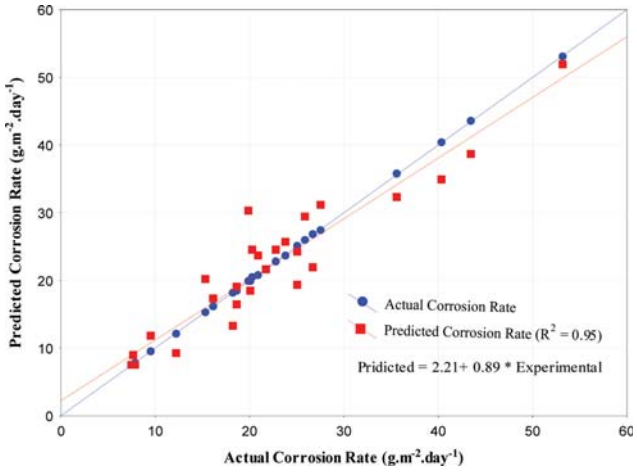

Fig. 1. Performance of the quadratic mathematical model.

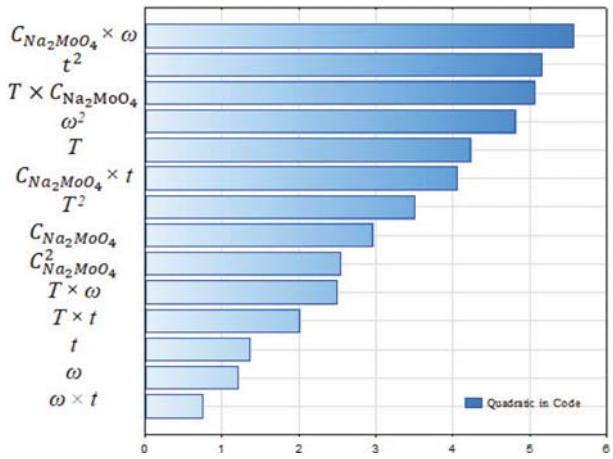

Fig. 2. Pareto chart for MC-steel in a saline solution containing nitrate and chloride ions.

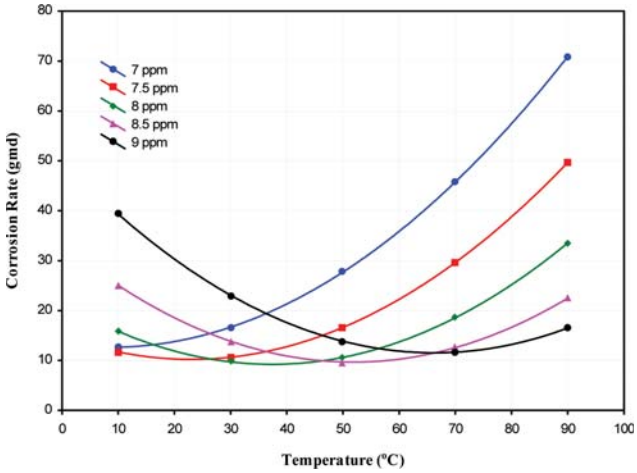

Fig. 3. Variety of predicted inhibited corrosion rate with temperature.

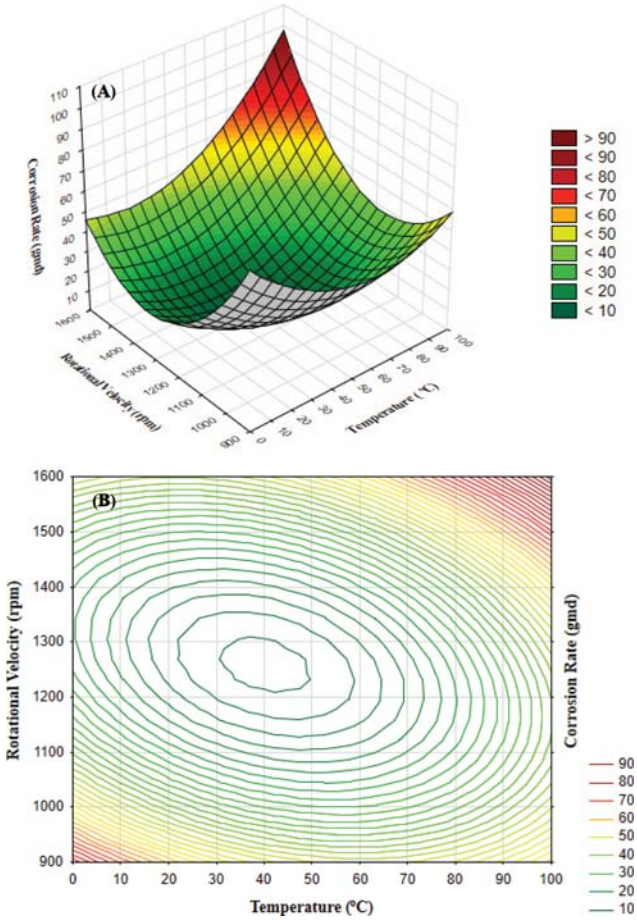

Fig. 4. Surface plot (A) and contour plot (B) of temperature and rotational velocity at the optimum conditions (8.09 ppm and 6.08 h) for corrosion rate of MC-steel.

coefficient. It can be used to assess the predicted rate of inhibited corrosion as a function of any factor [26,27]. For example, $C.R_{p(W,L)} = f(T)_{C,w,t}$ rate of inhibited corrosion rate as a function of temperature at constant concentration of inhibitor, optimum conditions of rotational velocity 1,257.45 rpm and exposure time 6.08 h. Fig. 3 shows the variation of corrosion rate with temperature at different inhibitor concentrations.

Another graphical representation of Eq. (3a) and (3b) is 3-dimensional and 2-dimensional curves, respectively. Fig. 4(A) and (B) shows the corrosion rate variation as a function of the temperature and the rotational velocity at optimum conditions. It can be seen that corrosion rate was significantly affected by rotational velocity and temperature, which agrees with the results of Cedeno et al. [28]. Similar figures can be obtained for other effects. Fig. 5(A) and (B) demonstrates the synergistic effect between temperature and exposure time on corrosion rate of steel at optimum conditions of inhibitor concentration and rotational velocity (8.09 ppm and 1,257.45 rpm). While, Fig. 6(A) and (B) represents the corrosion rate development as a function of the rotational velocity and the exposure time. Thus, the two-dimensional contour and three-dimensional response surface plots are the graphical representations of the mathematical equations used to evaluate the optimum conditions of the factors within the ranges considered [29]. It is clear from Figs. 4(A), 5(A), and 6(A) that the corrosion rate decreases, reaches a minimum, and then increases with the increase in the levels of the variables under consideration. The bottom of the response plot gives the minimum corrosion rate. The contours can aid in the forecast of the responses for any zone of the experimental domain and perform a very significant role in the study of a response surface. The contour plots are shown in Figs. 4(B), 5(B), and 6(B). Each contour curve denotes an infinite number of value combinations of two test variables derived from the quadratic model within the measured range. The minimum predicted value is recognized by the surface limited in the least circle or ellipse of the contour plot. The elliptical contour diagram specifies that the interactions between the corresponding factors are significant, while the circular contour plot indicates that the interactions between the corresponding factors are negligible [30]. These results agree with results of the Pareto chart. Moreover, a contour diagram is shaped to show the region of the optimum conditions visually. For quadratic response surfaces, such diagrams can be more complex compared to the simple series of parallel lines that can occur with first-order empirical relationships.

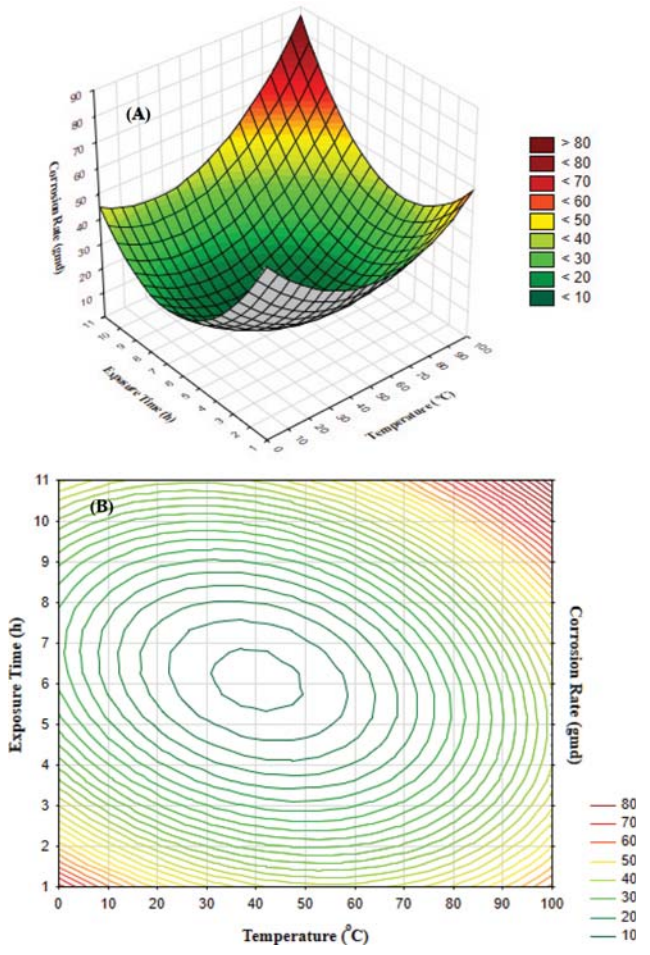

Fig. 5. Surface plot (A) and contour plot (B) of temperature and exposure time at the optimum conditions (8.09 ppm and 1,257.45 rpm) for corrosion rate of MC-steel.

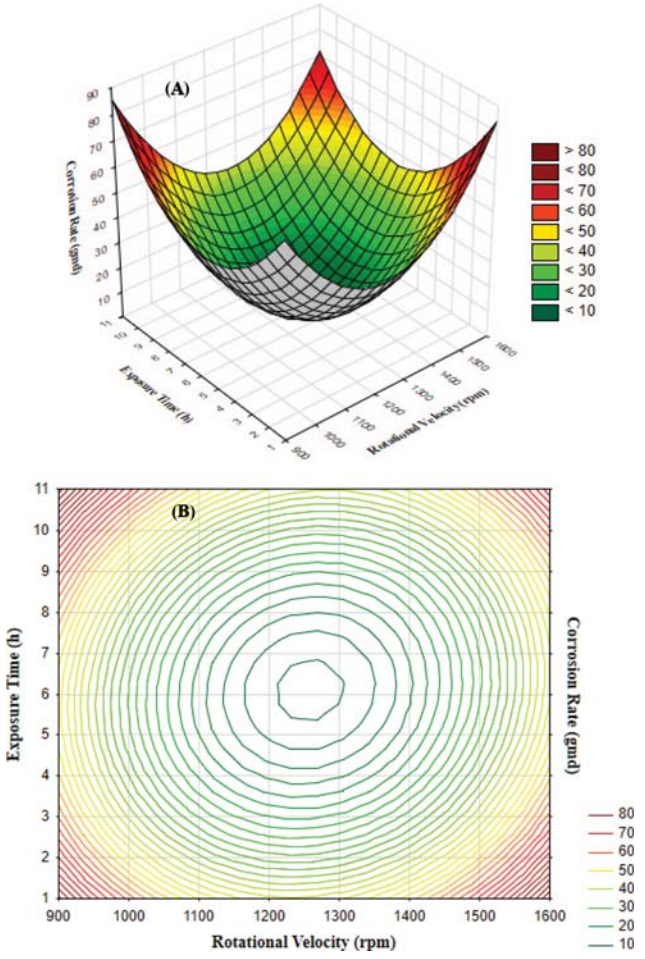

Fig. 6. Surface plot (A) and contour plot (B) of rotational velocity and exposure time at the optimum conditions (40.27 °C and 8.09 ppm) for corrosion rate of MC-steel.

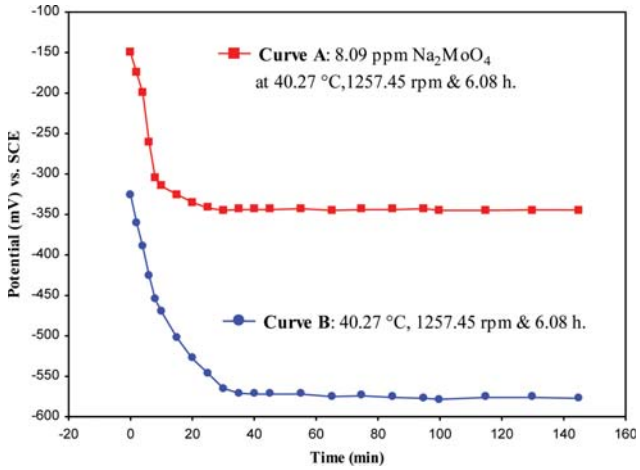

Fig. 7. Free corrosion potential for the MC-steel corrosion at the optimum conditions in presence (Curve A) and absence (Curve B) of Na_2MoO_4.

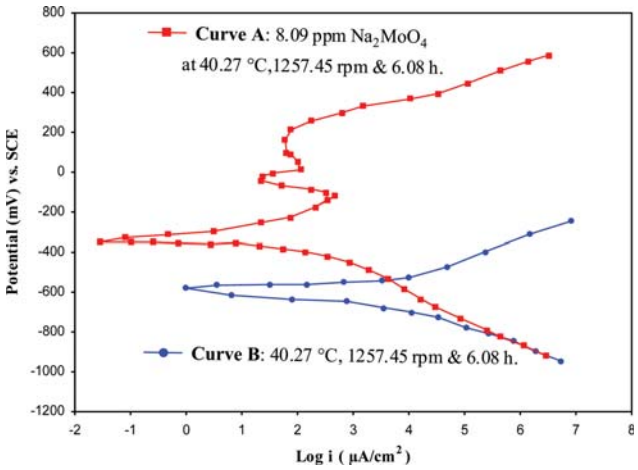

Fig. 8. Polarization curves for the MC-steel corrosion in aerated saline water containing 0.5 M $NaNO_3$ & 0.5 M NaCl ions at the optimum conditions. Curve A: inhibited water with Na_2MoO_4. Curve B: uninhibited water.

3. Open Circuit Potential (OCP) Measurements

OCP can afford significant information about the behavior of steel corrosion. The variation of the open circuit potential of MC-steel alloy with the immersion time in a saline water containing 0.5 M $NaNO_3$ & 0.5 M NaCl in absence and presence of 8.09 ppm Na_2MoO_4 at 40.27 °C, 1,257.45 rpm and 6.08 h has been studied. As shown in Fig. 7, the free corrosion potential shifts to more positive value in the presence of Na_2MoO_4 (Curve A). After one-hour immersion the steady state potential was recorded in the presence and absence of Na_2MoO_4; it was approximately −344.3 and −576 mV, respectively, relative to saturated calomel electrode. Many factors, such as, oxygen, chloride concentration, and electrolyte may affect the open circuit potential data. A higher probability of corrosion is expected with more negative reading of OCP. Evaluation of metal corrosion from the (absolute) free corrosion potential values may mislead engineers and cause errors in judgment if other factors are not considered. It must be stressed that the free corrosion potential measurement only reveals the corrosion probability at a given location and time. It is evident that long-term monitoring of the free corrosion potential reading is more meaningful. The reason for this variation with time depends and is affected by many parameters (i.e., material purity, surface treatment, oxygen contact …) [31].

4. Potentiodynamic Polarization Measurements

Polarization measurement was performed in an aerated, saline water containing nitrate and chloride ions (0.5 M $NaNO_3$ and 0.5 M NaCl) at the weight loss optimum conditions in absence and presence of sodium molybdate (SM) as an inhibitor at a temperature of 40.27 °C, 8.09 ppm of SM concentration, rotational velocity 1,257.45 rpm and exposure time of 6.08 h. Fig. 8 shows potentiodynamic polarization curves. From these curves, the kinetics electrochemical parameters, such as, corrosion potential (E_{corr}), corrosion current density (I_{corr}), and Tafel slopes (β_c and β_a) were obtained and presented in Table 5. The linear polarization resistance (R_p) can be evaluated from the Stern and Geary equation [32]:

$$R_p = \frac{\beta_a \beta_c}{2.303 I_{corr}(\beta_a + \beta_c)} \tag{9}$$

where R_p is a linear polarization resistance in ($\Omega \cdot cm^2$), I_{corr} is the current density of corrosion ($\mu A/cm^2$), β_a and β_c are the Tafel slopes in (mV/dec) for anodic and cathodic curves, respectively. The corrosion rate also can be expressed in terms of penetration rate using the following equation [33]:

$$\text{C.R (mpy)} = \frac{0.129 \times I_{corr} \times EW}{d} \tag{10}$$

where C.R (mpy) is corrosion rate in mils/year, EW is the equivalent weight of the corroding iron species (28 g/eq), and d is the density of the corroding iron species (7.87 g/cm^3). This form of corrosion rate unit may be useful in predicating equipment age. Another important parameter is the percentage inhibition efficiency (η %) at the optimum conditions that can be calculated by using the following [34]:

$$\%\eta = \frac{I_{corr} - I_{corr(inh)}}{I_{corr}} \times 100 \tag{11}$$

Table 5. The results of electrochemical corrosion in the aerated saline solution containing 0.5 M $NaNO_3$ & 0.5 M NaCl ions at the optimum corrosion inhibition rate

Case	OCP (mV) SCE	I_{corr} ($\mu A/cm^2$)	E_{corr} (mV) SCE	β_c (mV/dec)	β_a (mV/dec)	R_P ($\Omega \cdot cm^2$)	CR (mpy)	Efficiency η (%)
Inhibited	−344.3	36.87	−350	−62	84	27.88	16.92	95.90
Blank	−576	900	−580	−55	47	5.10	413.06	

where $I_{corr(inh)}$ and I_{corr} are the corrosion current densities in presence and absence of inhibitor, respectively. Both C.R (mpy) and percentage inhibition efficiency (η %) are collected in Table 5. With the presence of sodium molybdate (SM) inhibitor concentration, the corrosion current density decreased and the polarization resistance increased.

Fig. 8 shows that the effect of an anodic-type Na_2MoO_4 inhibitor (sometimes referred to as passivator) acts on the metal surface producing a large corrosion potential anodic shift. This shift forces the metallic surface into the passivation region. I_{corr} is reduced, while the E_{corr} shifts towards higher (more positive) values. The inhibitor can be categorized as cathodic or anodic when the change in the E_{corr} value is larger than 85 mV [35]. From Table 5, the maximum shift of E_{corr} value at optimum conditions was 230 mV, which is higher than the recommended value. This postulates that the SM corrosion inhibitor is adsorbed to large extent on anodic areas, which slows the main anodic reaction of the steel dissolution. It is also clear from Table 5 that the current corrosion density is reduced in the presence of inhibitor. Correspondingly, η % value is high, which indicates the excellent performance of the inhibitor. Furthermore, no significant changes were detected in the Tafel slope of cathodic region (β_c) value in polarization curve, while the anodic one (β_a) was significantly affected. This suggests that there was no change mechanism of cathodic reaction. The effect was more pronounced with anodic corrosion mechanism in the presence of the inhibitor.

CONCLUSIONS

The effects of the sodium molybdate inhibitive action and corrosion behavior of MC-steel in saline water at different conditions of temperature, inhibitor concentration, rotational velocity and the exposure time were investigated. Experimental design was used to construct the weight loss tests, and a mathematical model was suggested. The effect of independent variables on corrosion rate follows the sequence of temperature, then inhibitor concentration, exposure time, and rotational velocity. Mathematical model was useful in evaluating of optimum conditions. Generally, the results of the model are in good agreement with the experimental data. Steady-state open circuit potential was approached after one hour. Open circuit potential measurements showed that the steady state potential was reached after one hour of immersion time. Polarization studies showed that sodium molybdate (VI) was an anodic-type inhibitor. Corrosion current density decrease and corrosion potential shifted to more positive direction. Optimum inhibition efficiency was 95.9%, which indicates the high performance of sodium molybdate.

ACKNOWLEDGEMENT

The author would like to thank Department of Chemical Engineering/University of Technology/Baghdad/Iraq for support.

NOMENCLATURE

a_o, a_1, …, a_{14} are constants symbol for the model
C.R is the corrosion rate in g/m^2·day [gmd]
k represent
s the number of variables
t is exposure time [h]
T is temperature of saline water [°C]
Where $C_{Na_2MoO_4}$ is inhibitor concentration [ppm]
x_1 is temperature symbol for the model [°C]
x_2 is inhibitor concentration symbol for the model [ppm]
x_3 is rotational velocity symbol for the model [rpm]
x_4 is exposure time symbol for the model [h]
y_p is predicted corrosion rate for the model [gmd]
ω is rotational velocity [rpm]

REFERENCES

1. D. Oluyemi, O. Oluwole and B. Adewuyi, *Mater. Res.*, **14**, 135 (2011).
2. A. Oluwaseun and I. Simeon, *Inter. Jr. Eng. Res. Gen. Sci.*, **3**, 1141 (2015).
3. S. Ghareba and S. Omanovic, *Corros. Sci.*, **52**, 2113 (2010).
4. A. Khadom, A. Yaro, A. Kadum, A. AlTaie and A. Musa, *Am. J. Appl. Sci.*, **6**, 1409 (2009).
5. A. Khadom and K. Hameed, *Int. J. Chem. Technol.*, **4**, 17 (2012).
6. A. Mahmood and A. Khadom, *J. Fail. Anal. Preven.*, **16**, 1071 (2016).
7. A. Fadhil, A. Khadom, H. Liu, C. Fu, J. Wang, N. Fadhil and H. Mahood, *J. Mol. Liq.*, **276**, 503 (2019).
8. S. Ahmed, W. Ali and A. Khadom, *J. Bio-and Tribo-Corrosion*, **5**, 15 (2019).
9. J. Trela and M. Scendo, *Ochrona Przed Korozia*, **55**, 224 (2012).
10. A. Khadom, B. Abod, H. Mahood and A. Kadhum, *J. Fail. Anal. Prev.*, **18**, 1300 (2018).
11. X. Zhao, J. Yang and X. Fan, *Appl. Mech. Mater.*, **44/47**, 4066 (2011).
12. J. Trela, M. Chat and M. Scendo, *CHEMIK*, **69**, 592 (2015).
13. T. Joanna, C. Milena and S. Mieczystaw, *CHEMIK*, **69**, 599 (2015).
14. D. Silva, A. Mirapalheta, C. Martinez-Huitle and J. Tonholo, *Int. J. Eng. Technol.*, **14**, 113 (2014).
15. G. Bueno, M. Taqueda, H. De Melo and I. C. Guedes, *Brazilian J. Chem. Eng.*, **32**, 177 (2015).
16. D. Bingol and S. Zor, *Corrosion*, **69**, 462 (2013).
17. B. Nikrooz, H. Ebrahimifar and M. Zandrahimi, *Indian J. Chem. Technol.*, **24**, 162 (2017).
18. D. Granato, V. De Araujo Calado and B. Jarvis, *Food Res. International*, **55**, 149 (2014).
19. B. Deniz and Z. Sibel, *Corrosion*, **69**, 467 (2013).
20. A. Khadom and K. Rashid, *World J. Eng.*, **15/3**, 388 (2018).
21. L. Tarantino, *Design and Analysis of Industrial Experiments*, Tetra Pak (2010).
22. P. Marcus and F. Mansfeld, Analytical Methods in Corrosion Science and Engineering, 10th Ed., Taylor and Francis Group, New York (2006).
23. A. Khadom, *Korean J. Chem. Eng.*, **30**, 2204 (2013).
24. C. Jeff Wu and S. Michael, Experiments: Planning, Analysis and Optimization, 2nd Ed., John Wiley New York, USA (2009).
25. A. Y. Musa, A. A. Kadhum, A. B. Mohamad, A. R. Daud, M. S. Takriff and S. K. Kamarudin, *Corros. Sci.*, **51**, 2393 (2009).
26. A. Yaro, H. Al-Jendeel and A. Khadom, *Desalination*, **270**, 193 (2011).
27. K. Rashid and A. Khadom, *Anti-Corrosion Methods and Materials*, **65**, 514 (2018).

28. M. Cedeno, L. Vera and T. Pineda, *J. Phys.: Conf. Series*, 786 (2017).
29. L. Zhao, Y. He, X. Deng, G. Yang, W. Li, J. Liang and Q. Tang, *Molecules*, **17**, 3618 (2012).
30. D. Thirumalaikumarasamy, V. Balasubramanian and S. Sabari, *J. Magnesium Alloys*, **5**, 133 (2017).
31. A. Musa, A. Kadhum, A. Mohamad, A. Daud, M. Takriff and S. Kamarudin, *Corros. Sci.*, **51**, 2393 (2009).
32. A. Yaro and A. Kahdom, *Int. J. Surf. Sci. Eng.*, **4**, 438 (2010).
33. H. Uhlig and R. Winston, Corrosion and Corrosion Control, 4th Ed., Wiley (2008).
34. A. Shams El Din, R. Mohammed and H. Haggag, *Desalination*, **114**, 95 (1997).
35. F. De Souza, *Corros. Sci.*, **51**, 642 (2009).